Glycoconj J (2014) 31:523–535
DOI 10.1007/s10719-014-9550-x

9-*O*-acetylated sialic acids differentiating normal haematopoietic precursors from leukemic stem cells with high aldehyde dehydrogenase activity in children with acute lymphoblastic leukaemia

Suchandra Chowdhury · Sarmila Chandra · Chitra Mandal

Published online: 5 October 2014

Abstract Childhood acute lymphoblastic leukaemia (ALL) originates from mutations in haematopoietic progenitor cells (HPCs). For high-risk patients, treated with intensified post-remission chemotherapy, haematopoietic stem cell (HSC) transplantation is considered. Autologous HSC transplantation needs improvisation till date. Previous studies established enhanced disease-associated expression of 9-*O*-acetylated sialoglycoproteins (Neu5,9Ac_2-GPs) on lymphoblasts of these patients at diagnosis, followed by its decrease with clinical remission and reappearance with relapse. Based on this differential expression of Neu5,9Ac_2-GPs, identification of a normal HPC population was targeted from patients at diagnosis. This study identifies two distinct haematopoietic progenitor populations from bone marrow of diagnostic ALL patients, exploring the differential expression of Neu5,9Ac_2-GPs with stem cell (CD34, CD90, CD117, CD133), haematopoietic (CD45), lineage-commitment (CD38) antigens and cytosolic aldehyde dehydrogenase (ALDH). Normal haematopoietic progenitor cells ($ALDH^+SSC^{lo}CD45^{hi}$Neu5,9Ac_2-$GPs^{lo}CD34^+CD38^-CD90^+CD117^+CD133^+$) differentiated into morphologically different, lineage-specific colonies, being crucial for autologous HSC transplantation while leukemic stem cells ($ALDH^+SSC^{lo}CD45^{lo}$Neu5,9Ac_2-$GPs^{hi}CD34^+CD38^+CD90^-CD117^-CD133^-$) lacking this ability can be potential targets for minimal residual disease detection and drug-targeted immunotherapy.

Keywords 9-O-acetylated sialoglycoproteins · Aldehyde dehydrogenase · Childhood acute lymphoblastic leukaemia · Autologous bone marrow transplantation · Haematopoietic precursor cells · Leukemic stem cells

Introduction

Acute lymphoblastic leukaemia (ALL), a malignant transformation of lymphoblasts, represents the commonest form of paediatric cancer [1, 2]. High-risk ALL patients treated with intensified post-remission chemotherapy are considered for allogeneic haematopoietic stem cell (HSC) transplantation [3].

Graft-*versus*-host disease (GVHD), a major complication of allogeneic HSC transplantation [4], avoided by autologous transplantation, has failed to enhance outcome in paediatric ALL [2]. Therefore, an urgent need exists for improvisation of autologous bone marrow (BM) transplantation with functionally normal haematopoietic progenitor cells (HPCs). Exploration for a universal marker for HPCs still exists.

Neuraminic/sialic acids (Sia), important cell membrane constituents, influence biological reactions. A variation of Sias is *O*-acetylation at C-9 position [5, 6]. Neoplastic transformation is characterized by increased cell surface Sia density [7, 8]. Exploring the preferential affinity of Achatinin-H, purified from *Achatina fulica*, towards linkage-specific *O*-acetylated Sias [7–11], we have identified an enhanced disease-associated expression of cell surface 9-*O*-acetylated sialoglycoproteins (Neu5,9Ac_2-GPs) on lymphoblasts of diagnostic ALL patients [7, 8, 12–18]. Reduced expression of

S. Chowdhury · C. Mandal (✉)
Cancer Biology and Inflammatory Disorder Division, Council of Scientific and Industrial Research-Indian Institute of Chemical Biology, 4, Raja S. C. Mullick Road, Jadavpur, Kolkata 700 032, India
e-mail: chitra_mandal@yahoo.com

S. Chandra
Clinical Haematology Service, 4, Gorky Terrace, Kolkata 700 017, India

these molecules on lymphocytes of children in clinical remission (CR) increased prior to and during relapse [16, 19].

With this background, we tried to identify a functionally normal HPC population from the BM of diagnostic patients, using the differential expression of Neu5,9Ac_2-GPs as a biomarker.

Here we have identified a normal HPC population from the BM of diagnostic ALL patients, by high cytosolic activity of aldehyde dehydrogenase ALDH ($ALDH^{hi}$) [20–22], along with positive cell surface expression of stem cell antigens (CD34, CD90, CD117, CD133) and negative expression of the lineage-commitment antigen (CD38) [23–25]. Incidentally, this non-malignant population [26–28], expressing high leukocyte common antigen ($CD45^{hi}$) and less Neu5,9Ac_2--GPs, formed mixed colonies *in vitro* in methylcellulose-based medium demonstrating their functionally normal character. Lineage composition analysis of these colonies showed their ability to differentiate *in vitro*. However, this population was absent in diagnostic peripheral blood (PB), indicating that the HPCs ideal for autologous BM transplantation resides in the BM microenvironment.

Simultaneously, another co-existing $ALDH^{hi}$ population was evident, with positive expression of CD34 and CD38 and negative expression of CD90, CD117 and CD133. This population in the $CD45^{lo}$ region showed higher expression of Neu5,9Ac_2-GPs indicating that they might be the leukemic stem cells (LSCs). Taken together, future studies on these HPCs and LSCs will help in deciphering the biology of childhood ALL.

Materials and methods

Clinical samples

PB and BM samples were obtained from children newly diagnosed for ALL (PB_{ALL}, n=16 and BM_{ALL}, n=26). The study population comprised of males and females (2:1) with median age (6 years; range 0.8–16 years) and median presenting white blood cell count (12×10^9/L, range 0.4–$1{,}000\times10^9$/L) obtained from Kothari Medical Centre, Kolkata. All samples were processed within a day of collection of samples. Controls included PB and BM samples from children in clinical remission (CR, PB_{CR}, n=5 and BM_{CR}, n=8).

Diagnosis was established by cytological examination of BM smears according to French-American-British Group recommendations, belonging to L1 or L2 and by cytogenetic study. Each sample was immunophenotyped by flow cytometry using a standard panel of monoclonal antibodies (mAbs). These patients concurrently showed high expression of Neu5,9Ac_2-GPs on lymphoblasts, based on their binding with flourescein isothiocyanate (FITC) conjugated Achatinin-H [13–16, 19, 20] and high intensity of anti-Neu5,9Ac_2-GPs antibodies in their serum [16, 17, 29]. The Institutional Human Ethical Committee approved the study. Consent was taken from the parents and/or guardian of the diseased children for the samples.

Sample preparation

Mononuclear cells (MNCs) from clinical samples (PB/BM) were separated by Ficoll-Hypaque density gradient centrifugation, washed and suspended in RPMI-1640 supplemented with 2 % foetal calf serum, 2 mM glutamine and gentamycin (Medium A).

Aldefluor assay and immunophenotyping by flow cytometry

Viable MNCs expressing cytosolic ALDH were isolated by flow cytometry (FACSCalibur, Becton Dickinson) using Aldefluor reagent system (StemCell Technologies Inc, Canada) [20]. For immunophenotyping, MNCs were stained with other fluorescent conjugated mAb and with FITC-Achatinin-H for 1 h, on ice, centrifuged at 2,000 rpm for 5 min. Each cell pellet was suspended in Aldefluor assay buffer (0.5 ml). Analysis and calculations were performed using CellQuestPro software (BD Biosciences, USA).

The panel consisted of FITC–, PE–, PE-CY5– or APC–conjugated anti-CD45, anti-CD34, anti-CD90, anti-CD117, anti-CD38, CD10, anti-CD19, anti-CD7, anti-CD3, anti-CD4, anti-CD8, anti-CD56, anti-CD14, anti-CD13 and anti-CD33 (BD Biosciences) and PE-CD133 (Miltenyi Biotec, Germany).

Immunomagnetic separation and cell sorting

Progenitor populations were enriched using immunomagnetic separation technique, initially by negative selection, followed by positive selection of $CD34^+$ cells. Lineage negative cells (Lin^-) were obtained using StemSep® enrichment Cocktail (100 μL/ml cells) on a magnetic column (Stemcell Technologies). Briefly, MNCs ($2–8\times10^7$ cells/ml) were incubated with this cocktail on ice for 30 min; magnetic colloid (60 μl/ml) was added, mixed and incubated on ice for 30 min. Negative selection column was primed, inserted into green magnet and samples were loaded. The flow-through contained HPCs highly enriched in $CD34^+CD38^-$ population. $CD34^+$ cells were further enriched using a positive-selection magnetic column. Lin^- cells were initially labelled with anti-CD34 antibody and processed as above. The purity of the separated fraction was assessed by flow cytometry using PE-CD34 along with the aforesaid panel of mAbs.

Lin^-CD34^+ populations were stained for PE-CD45 and ALDH. Labelled cells were further sorted to isolate more specific phenotypes using the cell sorter of FACS. $Lin^-CD34^+ALDH^+$ and $Lin^-CD34^+ALDH^+CD45^{hi}$

populations along with $Lin^+CD34^+ALDH^+CD45^{lo}$ population were independently sorted.

Confocal microscopy

Co-localization of intracellular ALDH in $CD45^{hi}$ lymphocytes were visualized in $Lin^-CD34^+ALDH^+CD45^{hi}$ sorted population. Briefly, the washed cells in phosphate buffered saline (1×10^5 cells/50 μl of PBS) were allowed to adhere onto poly-L-lysine pre-coated cover slips at 25 °C for 1 h. Cells were fixed with 1 % paraformaldehyde (PFA, 100 μl) for 30 min on ice, incubated with ammonium chloride (50 mM, 100 μl), washed with PBS and mounted on glycerol in PBS (1:1) containing 1,4-diazabicyclo [2.2.2] octane (0.02 g) and analysed. Slides were analysed for FITC and PE probes using 488 nm laser, under a confocal scanning microscope (Leica SP2, Wetzlar, Germany).

Haematopoietic progenitor colony assays and morphological identification

Sorted populations containing Lin^-, Lin^-CD34^+, $Lin^-CD34^+ALDH^+$, $Lin^-CD34^+ALDH^+CD45^{hi}$ and $Lin^+CD34^+ALDH^+CD45^{lo}$ cells were separately put into culture using methylcellulose-based medium (METHOCULT® GF H4434, Stem Cell Technologies) to determine the number of colony forming unit-erythroid (CFU-E), burst forming unit-erythroid (BFU-E), CFU-granulocyte and macrophage (CFU-GM), CFU-granulocyte (CFU-G), CFU-macrophage (CFU-M) and CFU-granulocyte, erythrocyte, macrophage, megakaryocyte (CFU-GEMM). Assays were performed by plating ~1,000 viable cells/1.1 ml medium of each of these phenotypes, separately, in 35-mm tissue culture dishes and incubated without disturbance at 37 °C, 5 % CO_2, for 14–17 days. All cultures were maintained in triplicate.

Colonies were evaluated for morphologic characteristics and enumerated under light microscopy (Zeiss, Muenchen, Germany) following incubation. Colonies consisting of ~40 cells were counted. Plating efficiency, which is a measure of the number of colonies originating from single cells, was calculated for each of these sorted populations and expressed as percentage.

Colonies were isolated from the methylcellulose-bed, suspended in Medium A, washed, resuspended and used for the following flow-cytometric assays.

Colony lineage composition

Cells isolated from colonies were analysed to identify haematopoietic cells consisting of lymphoid, myeloid and erythroid lineages. Accordingly, cells were stained with fluorochrome conjugated mAbs against various cell surface markers like the leukocyte common antigen (CD45), B-(CD10, CD19) and T-(CD3, CD7) lymphocytes, stem cell (CD34), lineage-commitment (CD38), monocytes (CD14), myeloid (CD33) and erythroid (Glycophorin A) antigens. The status of $Neu5,9Ac_2$-GPs was simultaneously investigated using Achatinin-H. All tubes were incubated with respective mAbs and/or lectin for 1 h at 4 °C, in dark, washed in PBS and fixed in 1 % PFA for flow-cytometric analysis.

Apoptosis in the colonies

To verify the presence of apoptotic population in the cells isolated from colonies, they were stained with FITC-annexin V (BD Biosciences) and propidium iodide. Cells (1×10^6/100 μl) were suspended in annexin-V binding buffer mixed with FITC-annexin V (5 μl) and propidium iodide (5 μl) and incubated for 30 min in the dark at 25 °C and processed.

DNA cell cycle analysis

Cells (5×10^5) were isolated from the colonies washed, suspended in Medium A and analysed for DNA ploidy using CycleTEST™ PLUS DNA Reagent Kit (BD Biosciences) as per manufacturers' instructions.

Statistical analysis

Statistical analysis was performed using Graph-Pad Prism statistics software program (Graph-Pad Software Inc., CA). Results expressed as Mean ± S.D. for individual set of experiments. Two-tailed p value (P) for student's t-test was considered significant for $P<0.05$.

Results

BM_{CR} samples were used as control while BM_{ALL} samples were used for identification and characterization of cells with high ALDH activity.

High ALDH activity identified mononuclear cells with immature cell morphology in BM_{CR}

To identify the $ALDH^+$ cells in BM_{CR} based on their scatter, two simultaneous dot-plots were drawn, one with forward scatter (FSC) *versus* side scatter (SSC) while the other with ALDH *versus* SSC (Fig. 1). MNCs from BM_{CR} in the former plot were gated R1 (Fig. 1a). DEAB control as shown in the latter plot (Fig. 1b) were gated R2 lacking $ALDH^+$ cells. In contrast, a subpopulation of cells with very high ALDH activity ($ALDH^+$) was visualized in MNCs of BM_{CR}, in R2 region (Fig. 1c). When superimposed by multiple gating, cells in R2 showed medium granularity (SSC^{lo}), indicating

stem/progenitor cells. These medium sized cells ($ALDH^+SSC^{lo}$) scattered between 400 and 600 in FSC (Fig. 1d), accounted for 0.58±0.24 % of MNCs in BM_{CR} (range 0.34–0.82 %; n=5) and were considered as normal HPCs. However, such population was absent in MNCs from PB_{CR} (n=5).

Identification of cells with high ALDH activity from BM_{ALL} and PB_{ALL} of patients

In search of $ALDH^+SSC^{lo}$ population from BM_{ALL} samples (n=8), MNCs gated as R1 (Fig. 1a) were analysed for ALDH activity (Fig. 2). In contrast to DEAB control (Fig. 2a), density-plot with ALDH *versus* SSC in BM_{ALL} revealed a significant population of MNC with high ALDH activity and medium SSC ($ALDH^+SSC^{lo}$, R2, Fig. 2b), accounting for 1.64±0.28 % of MNCs in BM_{ALL} (range 1.36–1.92 %).

Dot-plot with ALDH *versus* SSC (showing 1 % of total 1,00,000 events acquired) for DEAB control lacked cells in R2 (Fig. 2c). Similar plot for BM_{ALL} sample emphasized that these $ALDH^+SSC^{lo}$ cells (R2, red) have different scatter properties than cancerous lymphoblasts (green, Fig. 2d).

FSC scatter of this $ALDH^+SSC^{lo}$ population, using pseudo colour dot-plot, revealed two distinct populations in BM_{ALL} (Fig. 2e), in contrast to the single population in BM_{CR}. A less dense population, scattering within 400–600, was identical to that encountered in BM_{CR} *i.e.*, normal HPCs, while the denser one scattering within 600–1,000, may be leukemic stem cells (LSCs). The contour plot (Fig. 2f) attests to the finding in Fig. 2d, highlighting that the $ALDH^+$ cells have different scatter properties compared to the other lymphocytes.

Similar assay was performed with PB_{ALL} (n=8), where three patients had 0.28±0.22 % $ALDH^+SSC^{lo}$ cells (range 0.06–0.5 %), remaining lacking this population.

Phenotypic characterization of progenitor population, confirming the presence of both normal HPCs and LSCs in MNCs of BM_{ALL}

Following identification of $ALDH^+SSC^{lo}$ cells in BM_{ALL} (n=8), we investigated the status of other known CD antigens on this population. Accordingly, the status of CD45, CD34, CD90, CD117, CD133, CD38 and Neu5,9Ac_2-GPs in the $ALDH^+SSC^{lo}$ cells were analysed (Fig. 3). To reconfirm, the status of B-(CD10, CD19), T-(CD3, CD7, CD4, CD8), NK (CD56), monocyte (CD14) and myeloid (CD13, CD33) lineages, the status of the respective CD antigens were also assessed.

MNCs were initially gated R1 (Fig. 1a). In contrast to no $ALDH^+$ cells in DEAB control (Fig. 3a), the test sample had a distinct population of $ALDH^+$ cells gated R2 (Fig. 3b). Normal haematopoietic cells have higher expression of CD45, compared to cancerous lymphoblasts [26–28, 30]. To assess the scatter of $ALDH^+$ cells in $CD45^+$ population, a dot-plot with CD45 *versus* SSC was drawn, superimposing multiple gating ($ALDH^+$ cells). $ALDH^+$ cells scattered in both $CD45^{lo}$ and $CD45^{hi}$ population, gated R3 and R4 respectively (Fig. 3c). Since lower expression of CD45, expressed in terms of mean fluorescence intensity (MFI), confirmed MNCs as cancerous in contrast to normal lymphocytes, the $ALDH^+CD45^{lo}$ population may be considered as LSCs (0.6–0.8 %) while the $ALDH^+CD45^{hi}$ population might be normal HPCs (0.3–0.5 %).

After establishing the differential expression of Neu5,9Ac_2-GPs in ALL, being high in malignant lymphoblasts and low in normal lymphocytes, we explored their expression in $ALDH^+$ cells. A dot-plot with Achatinin-H *versus* CD45, using multicolour gating, revealed LSCs (R3) as $CD45^{lo}$Neu5,9Ac_2-GPs^{hi} and HPCs (R4) as $CD45^{hi}$Neu5,9Ac_2-GPs^{lo} (Fig. 3d). MFI of Neu5,9Ac_2-GPs^{lo} in $ALDH^+SSC^{lo}$ population was <100 arbitrary units (au) while that of Neu5,9Ac_2-GPs^{hi} was >100 au.

To confirm the primitive nature and lack of lineage-commitment, the scatter properties of LSCs and HPCs were analysed in dot-plot comprising CD34 *versus* CD38. The LSCs (R3) were $CD34^+CD38^+$ while the HPCs (R4) were $CD34^+CD38^-$ (Fig. 3e). Thus the HPCs were more primitive than the LSCs. When assessed for the presence of CD90, CD117 and CD133, the $ALDH^+SSC^{lo}CD45^{hi}$Neu5,9Ac_2-$GPs^{lo}CD34^+CD38^-$ HPC population (R4) was concurrently positive for all three while the $ALDH^+SSC^{lo}CD45^{lo}$Neu5,9Ac_2-$GPs^{hi}CD34^+CD38^+$ LSC population (R3) was negative for the same (Fig. 3f-h).

Therefore, as per our finding, normal HPCs among leukemic blasts had the phenotype of $ALDH^+SSC^{lo}CD45^{hi}$Neu5,9Ac_2-$GPs^{lo}CD34^+CD38^-CD90^+CD117^+CD133^+$ while the phenotype $ALDH^+SSC^{lo}CD45^{lo}$Neu5,9Ac_2-$GPs^{hi}CD34^+CD38^+CD90^-CD117^-CD133^-$ represented the LSCs. The $ALDH^+SSC^{lo}$ cells were negative for all the lineage-specific antigens substantiating their primitive nature (not shown in figure).

Similar assay was performed with PB_{ALL} (n=8) where LSCs were found in ~50 % of the analysed samples with insignificant number of HPCs. The BM_{CR} (n=3) samples, analysed for the same, showed only the presence of HPCs (0.4–0.7 %).

Enrichment of HPCs from MNCs of BM_{ALL} for *in vitro* culture

To isolate normal HPCs ($ALDH^+SSC^{lo}CD45^{hi}$Neu5,9Ac_2-$GPs^{lo}CD34^+CD38^-CD90^+CD117^+$ $CD133^+$) for *in vitro* clonogenic assay, MNCs from $BM_{ALL,}$ (n=4, gated R1, Fig. 4a), with 80±10 % $CD34^+$ cells (R2, Fig. 4b) were used; ~70 % of these were $CD34^+Lin^-$, remaining being

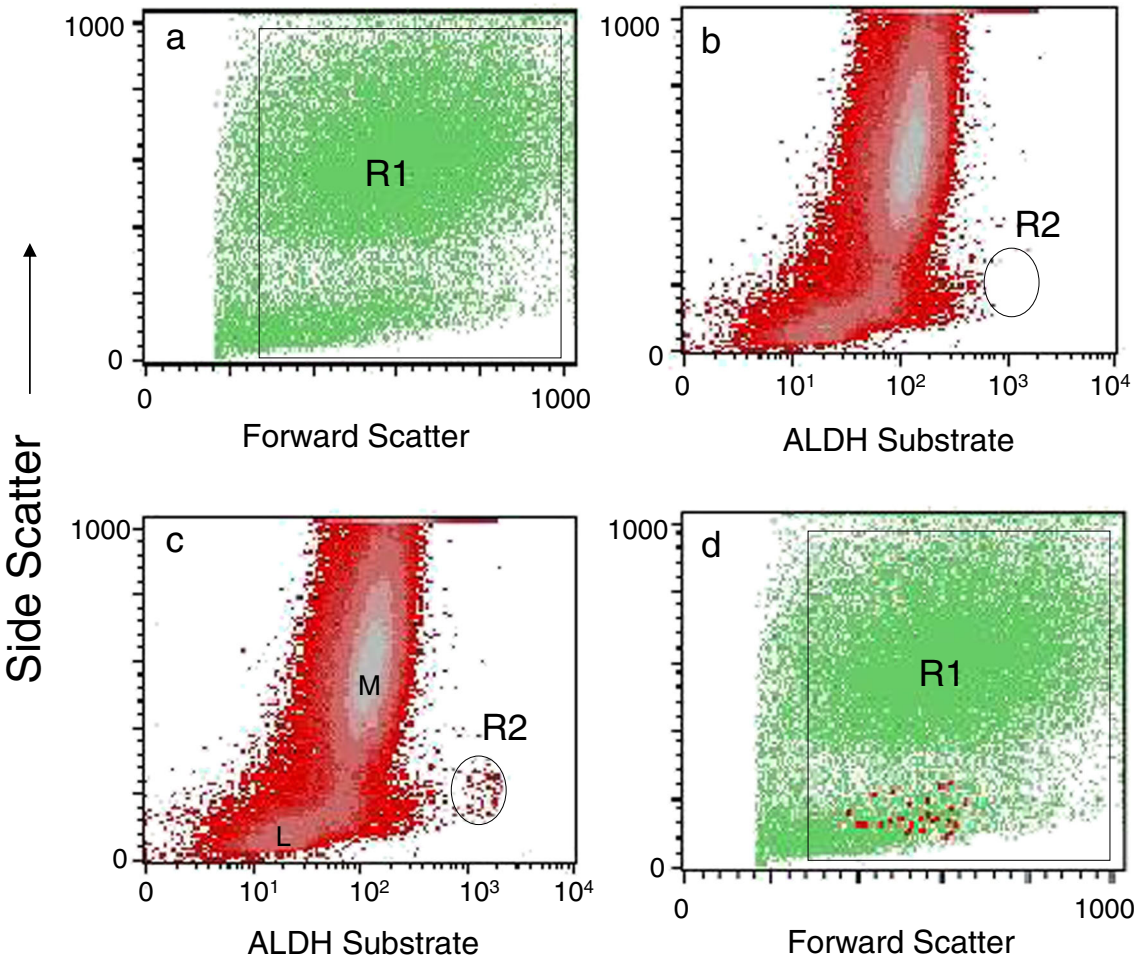

Fig. 1 High aldehyde dehydrogenase (ALDH) activity identifies cells with stem/progenitor cell morphology in bone marrow (BM_{CR}) sample of patients in clinical remission. Activated Aldefluor substrate (5 μl) was added to MNCs (1×10^6 cells), suspended in ALDEFLUOR assay buffer (1 ml) and thoroughly mixed. Half the cell suspension (0.5 ml) was transferred to a tube containing diethylaminobenzaldehyde (DEAB, 5 μl), a specific inhibitor of ALDH serving as control. Samples were incubated for 30 min at 37 °C for optimum enzyme activity. Data from a representative patient is shown. **a** Forward Scatter (FSC) *versus* Side Scatter (SSC) dot-plot is created, with region R1 drawn to encompass all nucleated cells. **b** Dot plot with FL1-H *versus* SSC shows control for Aldefluor assay. FL1 contains the DAAA, fluorescent substrate for ALDH, where, reaction has been blocked by DEAB. R2 is so gated that no events appear in this region. This setting served as control for subsequent analyses. **c** ALDH substrate, DAAA *versus* SSC dot plot for BM_{CR} sample gated on R1. R2 shows $ALDH^+SSC^{lo}$ cells. MNCs of BM_{CR}-ALDH staining exhibit a bright, low/medium SSC population that is extremely bright for ALDH substrate when compared with monocytes (M), lymphocytes (L), or debris. **d** When superimposed over the whole MNC population (*green*), $ALDH^+$ cells (*red*) show scatter characteristics of stem/progenitor cells

$CD34^+Lin^+$. These cells scattered in $ALDH^+CD45^{lo}$ (R3) and $ALDH^+CD45^{hi}$ (R4) regions respectively (Fig. 4c).

Lineage depletion resulted in 98.44 % reduction in lineage-committed cells. These Lin- cells were positively selected for $CD34^+$ cells. Following this, a defined population of $CD34^+CD38^-$ cells (98.3 % enrichment) was identified (R5, Fig. 4d), which was $ALDH^+CD45^{hi}$, having >96.41 % $ALDH^+$ cells and >98.33 % $CD45^+$ cells (Fig. 4e). An aliquot of this sorted $ALDH^+CD45^{hi}CD34^+CD38^-$ population was assessed for the presence of CD90, CD117, CD133 and $Neu5,9Ac_2$-GPs. These cells had very low expression of $Neu5,9Ac_2$-GPs (<5 %), was positive for all three stem cell antigens (>93.1 % $CD90^+$, >96.22 % $CD117^+$ and >97.27 % $CD133^+$, Fig. 4f). This $ALDH^+SSC^{lo}CD45^{hi}Neu5,9Ac_2$--$GPs^{lo}CD34^+$ $CD38^-CD90^+CD117^+CD133^+$ population was assayed for lineage specific antigens (CD19, CD10, CD33, CD3, CD14 and CD56). As expected this population was negative for all these markers (Fig. 4g) and accounted for 0.45–1.1 % of the total MNCs in BM_{ALL} which was enriched by 95 % post-sorting.

Co-localization of cytosolic ALDH and cell surface CD45

To ascertain the co-localization of cytosolic ALDH and cell surface CD45 in sorted HPC population, the Lin^-CD34^+ cells after being isolated by immunomagnetic

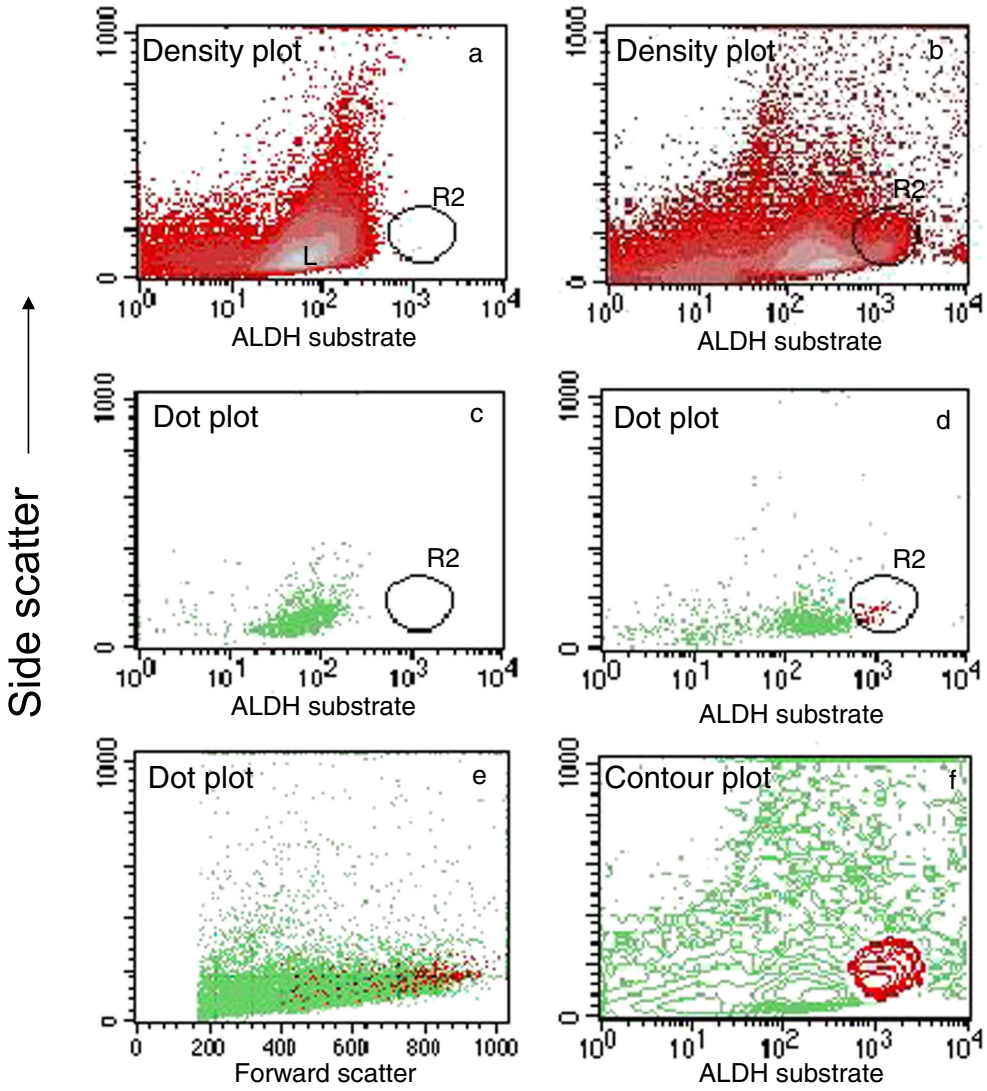

Fig. 2 Activity of ALDH in MNCs of bone marrow (BM_{ALL}) from child with ALL at diagnosis. MNCs from a representative patient, at diagnosis, were stained with ALDH as described in Materials and methods. Density plot with ALDH substrate *versus* SSC showing lack of $ALDH^+$ cells in R2 region of DEAB inhibited control (**a**). Similar dot plot showing presence of $ALDH^+$ population is BM_{ALL} (**b**). Dot plot of the data (shown in **a**), showing 1 % of the total events (1,00,000 events acquired), used as control for **d** (**c**). Dot plot of the data shown in **b**, showing the difference in scatter of $ALDH^+$ cells as compared to the lymphoblasts (**d**). When superimposed over the whole MNC population (*green*), $ALDH^+$ cells (*red*) show scatter characteristics of stem/progenitor cells (**e**). $ALDH^+$ cells shown in contour plot (**f**)

separation were assayed followed by visualization of the $Lin^-CD34^+ALDH^+CD45^{hi}$ population in confocal microscope. Intracellular ALDH activity was identified as a green ring in the cytosol while the cell surface CD45, appeared as a surrounding red ring (Fig. 4h) ensuring intact membrane architecture of this sorted population with ALDH activity.

Morphologically distinct colonies produced from *in vitro* culture

To investigate the functional characteristics of the immunomagnetically separated and cell sorted populations from MNCs of BM_{ALL} (n=6), clonogenic activity was assayed. Five different phenotypes of cells viz., Lin^-, Lin^-CD34^+, $Lin^-CD34^+ALDH^+$, $Lin^-CD34^+ALDH^+CD45^{hi}$ and $Lin^+CD34^+ALDH^+CD45^{lo}$ were independently put into culture. The colonies formed after 14–17 days were identified morphologically. Clonogenic progenitors namely, CFU-E, BFU-E, CFU-G, CFU-M, CFU-GM could be well identified while CFU-GEMM were absent.

$Lin^-CD34^+ALDH^+CD45^{hi}$ population from BM_{ALL} showed maximum proliferative capacity *in vitro*

To assess the sorted population with maximum potential to form *in vitro* colonies, the colonies produced from each viz., Lin^-, Lin^-CD34^+, $Lin^-CD34^+ALDH^+$, $Lin^-CD34^+ALDH^+CD45^{hi}$ and $Lin^+CD34^+ALDH^+CD45^{lo}$ were counted. Colonies produced from the sorted MNCs from BM_{ALL} of a representative diagnostic patient is shown in Table 1. While the colony types CFU-E, BFU-E, CFU-G, CFU-M and CFU-GM were formed in the first four studied

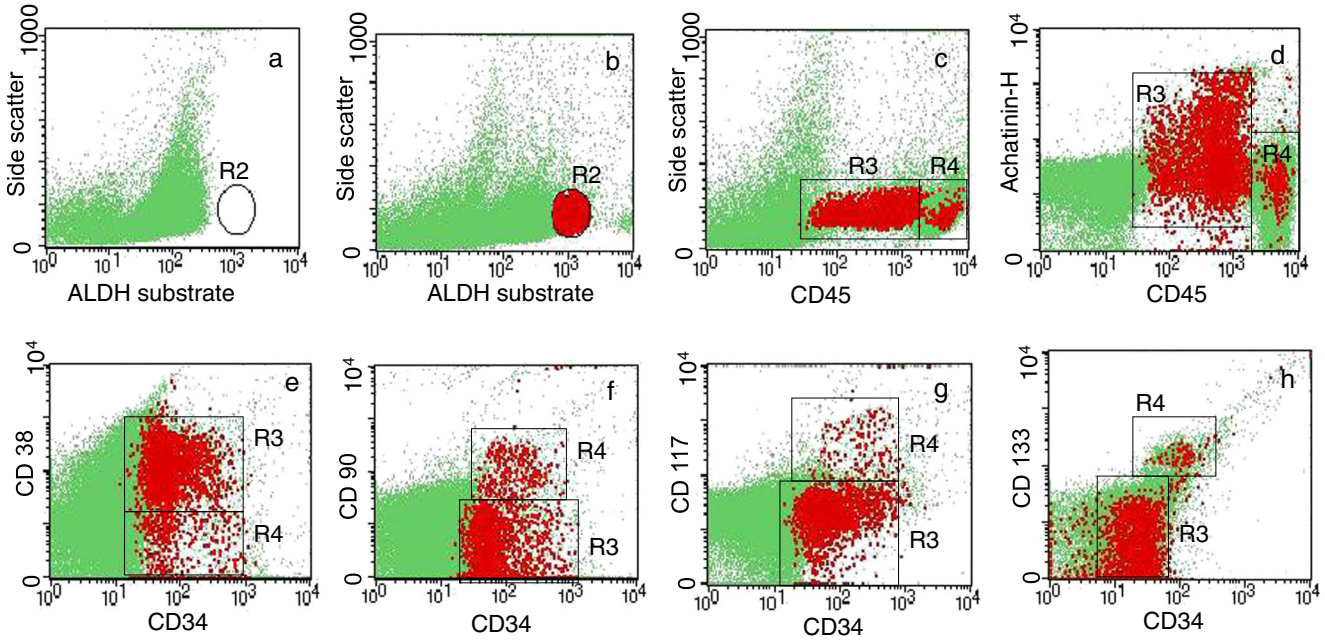

Fig. 3 Phenotypic characterization of ALDH$^+$ cells from diagnostic BM samples (BM_{ALL}). MNCs, stained with ALDH, were co-stained with mAbs specific to certain cell surface markers, as described in Materials and methods. Data from a representative patient is shown. Lymphoblasts were gated as R1 (not shown in figure). **a** DEAB control showing no ALDH$^+$ cells in R2 region. **b** ALDH$^+$ cells (*red*) shown in a dot plot comprising ALDH *versus* SSC. *Red dots* showing ALDH$^+$ cells have been highlighted to show their exact location; they do not represent the actual percentage of cells. Provided in the background is the MNC population (*green*). Pseudo-colour dot plots showing the subpopulations of ALDH$^+$ cells (*red*) in **c-h. c** Dot plot with CD45 *versus* SSC showing two distinct populations of ALDH$^+$ cells in CD45^{lo} and CD45^{hi} populations, shown as R3 and R4 respectively. **d** Achatinin-H *versus* CD45 profile showing two distinct populations of ALDH$^+$ cells, being Achatinin-H^{hi}CD45^{lo} and Achatinin-H^{lo}CD45^{hi}, shown as R3 and R4 respectively. **e** Dot plot with CD34 *versus* CD38, showing the profile of ALDH$^+$ cells in two distinct populations, CD34$^+$CD38$^+$ and CD34$^+$CD38$^-$ shown as R3 and R4 respectively. **f** CD34 *versus* CD90 profile showing two distinct populations of ALDH$^+$ cells, CD34$^+$CD90$^-$ and CD34$^+$CD90$^+$, shown as R3 and R4 respectively. **g** CD34 *versus* CD117 profile showing two distinct populations of ALDH$^+$ cells, CD34$^+$CD117$^+$ and CD34$^+$CD117$^-$, shown as R3 and R4 respectively. **h** CD34 *versus* CD133 profile showing two distinct populations of ALDH$^+$ cells, CD34$^+$CD133$^+$ and CD34$^+$CD133$^-$, shown as R3 and R4 respectively

phenotypes, CFU-GEMM was absent. However, the proliferative capacity of each of the populations varied significantly.

The Lin$^-$ cells showed minimum *in vitro* proliferation with a plating efficiency of 2 % (*i.e.*, 2 in 100 cells formed a single colony). Plating efficiency increased significantly ($P<0.0001$) in the wells plated with Lin$^-$CD34$^+$ cells (4.9 %) and was maximum using Lin$^-$CD34$^+$ALDH$^+$ cells (29.8 %). Colonies produced from Lin$^-$CD34$^+$ALDH$^+$CD45^{hi} cells showed insignificant variation from Lin$^-$CD34$^+$ALDH$^+$ population, confirming that the HPCs reside strictly in CD45^{hi} region. However, no colonies could be derived from Lin$^+$CD34$^+$ALDH$^+$CD45^{lo} population (Table 1).

The colony forming ability of the BM_{ALL} of six studied diagnostic patients did not vary significantly. The plating efficiencies of the different sorting populations were 2.7±1.4, 5.98±2.8, 28.5±5.4 and 28.6±5.6 in Lin$^-$, Lin$^-$CD34$^+$, Lin$^-$CD34$^+$ALDH$^+$ and Lin$^-$CD34$^+$ALDH$^+$CD45^{hi} respectively (Fig. 5). No morphologically different colonies could be seen in Lin$^+$CD34$^+$ALDH$^+$CD45^{lo} population.

Lineage content of colonies revealed stages of differentiation

To identify the phenotype of the morphologically different colonies formed from Lin$^-$CD34$^+$ALDH$^+$CD45^{hi} population, cells isolated from colonies were assessed for respective lineage specific antigens. Flow-cytometric analysis of these cells in the FSC *versus* SSC dot-plot revealed two distinct populations. The population in the lymphocyte region, having FSC within 400–600, was gated R1 (red) while another population in the debris region was gated R2 (grey, Fig. 6a). For the lineage content analysis, future studies were done on cells in R1 region, shown as red dots in the following dot-plots (Fig. 6b-h, j-k), while the grey dots showed the scatter of R2 region.

Initially, to assess the Neu5,9Ac_2-GPs content and the haematopoietic nature of the cells, they were plotted in a dot-plot with Achatinin-H *versus* CD45. Percentage of Neu5,9Ac_2-GPs$^+$ cells (4.1±2.8) was equivalent to the expression seen in MNCs from normal PB, having MFI of ~100 au (Fig. 6b), indicating that they were normal. More than >95 %

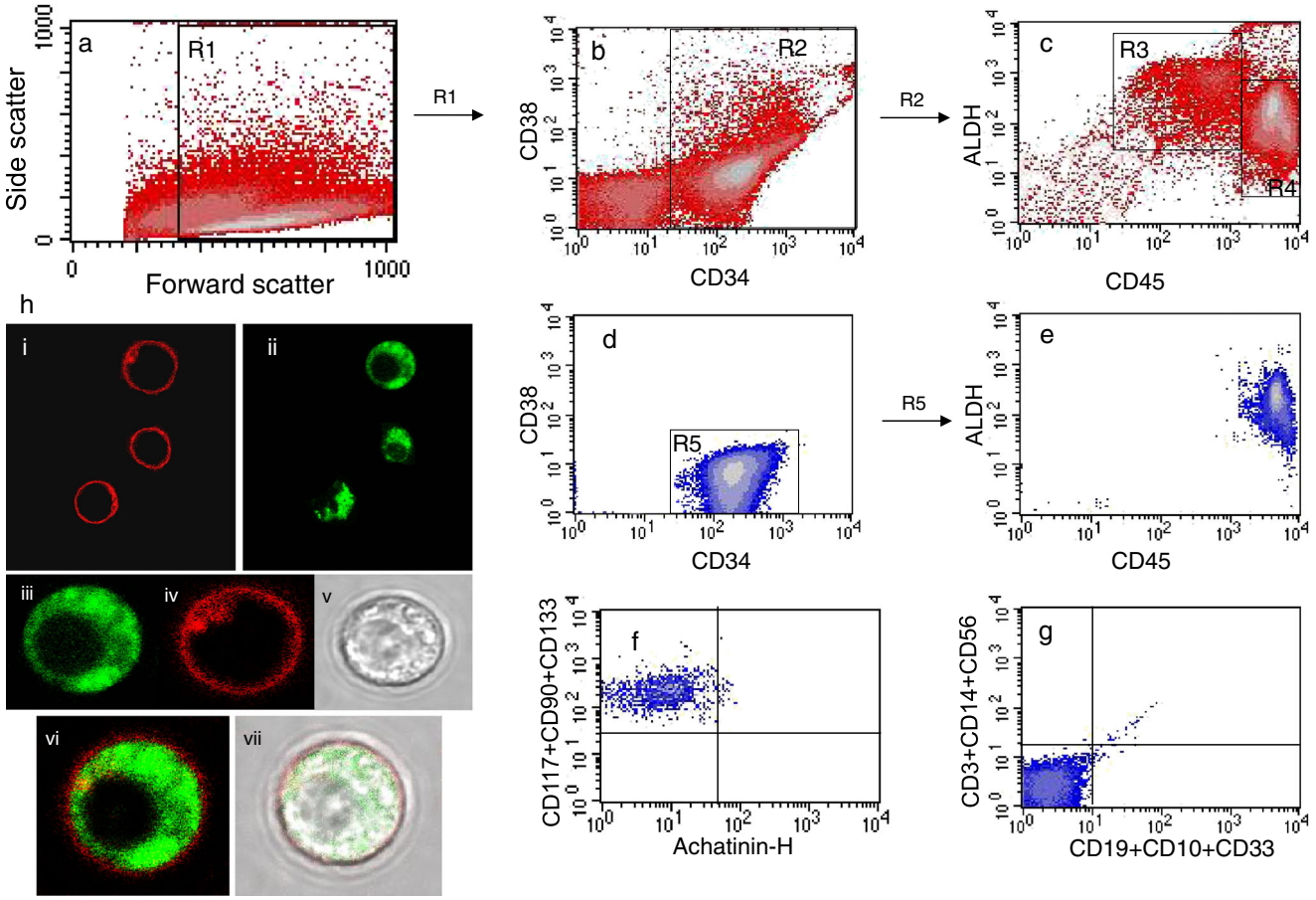

Fig. 4 Lineage composition of MNCs from diagnostic BM (BM_{ALL}) prior to and post sorting. MNCs, stained with ALDH, were co-stained with mAbs specific to certain cell surface markers, as described in Materials and methods. Figure represents data from a diagnostic patient. **a** FSC *versus* SSC dot plot is created, with region R1 drawn to encompass all nucleated cells. **b** Dot plot with CD34 *versus* CD38, gated on R1, show two distinct populations—$CD34^+CD38^+$ and $CD34^+CD38^-$, both of which was gated R2. **c** Cells in R2 comprise primarily of $ALDH^+CD45^{lo}$ and $ALDH^+CD45^{hi}$ populations, gated as R3 and R4 respectively. **d** After cell sorting, as described in Materials and methods, the $CD34^+CD38^-$ population is predominant, gated as R5. **e** Sorted $CD34^+CD38^-$ population (R5), analysed in a dot plot with CD45 *versus* ALDH, showed predominance of $ALDH^+CD45^{hi}$ population. This $CD34^+CD38^-ALDH^+CD45^{hi}$ population was put into culture. **f** An aliquot of $CD34^+CD38^-ALDH^+CD45^{hi}$ population was assessed for the presence of other stem cell antigens namely, CD90, CD117 and CD133 and also for Achatinin-H. **g** Another aliquot of the same was assessed for the presence of haematopoietic lineage specific antigens (CD19, CD10, CD33, CD3, CD14, CD56). **h** Confocal microcopy of $CD34^+CD38^-$ population is shown. The sorted cells were prepared for confocal microscopy as described in Materials and methods. Cells showing the (*i*) cell surface CD45 (*red*) and (*ii*) cytosolic ALDH (*green*). Single cell enlarged showing cytosolic ALDH (*iii*, *green*), Cell surface CD45 (*iv red*), phase contrast (*v*), overlay (*vi*) of cytosolic ALDH (*green*) and CD45 (*red*); overlay of cytosolic ALDH (*green*), CD45 (*red*) and phase contrast shown in (*vii*)

of the cells were $CD45^+$, with MFI ranging between 800 and 1,200 au, attesting to their normal immature lymphoblastic nature (Fig. 6b).

Dot-plot with CD34 *versus* CD38, for detecting the primitive ($CD34^+CD38^-$) and lineage-committed ($CD34^+CD38^+$ and $CD34^-CD38^+$) cells, revealed the presence of three cell types. Over 80 % cells were $CD34^+CD38^-$, while ~5 % were $CD34^+CD38^+$ and ~15 % were $CD34^-CD38^+$, indicating that most of the cells were still primitive while some were lineage-committed (Fig. 6c). Analysis of the B-lineage antigens revealed the absence of $CD10^+$ cells (0.9±0.8 %) and $CD19^+$ cells (0.7±0.6 %, Fig. 6d). The presence of T-lineage antigens was negligible in the cells, being 0.5–1 % positive for CD7 and CD3 (Fig. 6e-f). About 8 % cells were $CD33^+$ and 5 % were $CD14^+$ cells indicating the presence of monocytes (Fig. 6g). Erythroid progenitors were identified by the presence of 4–8 % Glycophorin A^+CD45^- cells (Fig. 6h). The column graph for the lineage status of these cells is shown in Fig. 6i.

The dot-plot with Annexin V and PI revealed that R1 is negative for these markers, indicating that the cells were alive while the cells in R2 region were found mostly expressing propidium iodide (Fig. 6j). DNA cell cycle analysis of the cells in R1 showed diploid and tetraploid peaks identical to that of normal lymphocytes (Fig. 6k).

On the contrary, colonies produced from $Lin^+CD34^+ALDH^+CD45^{lo}$ population retained the same phenotype confirming their LSC nature.

Table 1 Quantification of colony forming units (CFUs) in different sorted populations from a representative diagnostic bone marrow (BM_{ALL}) sample

Sorted populations	No of colonies per 10^3 cells						Total colonies	Plating efficiency (%)
	CFU-E	BFU-E	CFU-G	CFU-M	CFU-GM	CFU-GEMM		
Lin^-	3.33 (5,3,2)	1.33 (1,2,1)	5 (5,4,6)	1 (1,1,1)	10.33 (10,10,11)	0	20.99	2
Lin^-CD34^+	9 (10,8,9)	2 (1,3,2)	18.33 (18,18,19)	1 (0,2,1)	18.67 (19,20,17)	0	49	4.9
$Lin^-CD34^+ ALDH^+$	17.33 (17,17,18)	96.67 (89, 96, 105)	10.67 (12,10,10)	3.67 (4,3,4)	169.67 (134,177,198)	0	298.01	29.8
$Lin^-CD34^+ ALDH^+CD45^{hi}$	17.33 (15, 21,16)	92 (98, 86, 92)	10.67 (10,11,11)	3.67 (3,4,4)	170.33 (145, 189, 177)	0	294	29.4
$Lin^+CD34^+ ALDH^+CD45^{lo}$	0	0	0	0	0	0	0	0

Lineage depleted (Lin^-), Lin^-CD34^+, $Lin^-CD34^+ALDH^+$, $Lin^-CD34^+ALDH^+CD45^{hi}$ and $Lin^+CD34^+ALDH^+CD45^{lo}$ populations were sorted (using immunomagnetic separation technique and cell sorter of FACS) and cultured in semisolid methylcellulose media (Methocult H4434) as described in Materials and methods. Human progenitor colonies of erythrocyte (BFU-E, CFU-E) granulocyte (CFU-G), macrophage (CFU-M) and mixed lineages (CFU-GM, CFU-GEMM) were enumerated after 14–17 days of *in vitro* culture. Data represent the number of mean of individual colonies from the triplicate wells, produced per 1,000 cells plated for each of the sorted populations. The brackets show the individual counts of the triplicate. This data is obtained from a representative patient

Discussion

Identification of a functionally normal HPC population for autologous BM transplantation remains unsatisfactory due to lack of specific markers (phenotypic/functional). Our study for the first time identifies the presence of a distinct population of normal haematopoietic progenitor cells within the BM compartment of patients at diagnosis, exploring the differential expression of 9-*O*-acetylated sialic acids. These normal HPCs ($ALDH^+SSC^{lo}CD45^{hi}Neu5,9Ac_2$--$GPs^{lo}CD34^+CD38^-CD90^+CD117^+$ $CD133^+$) are functionally active and capable of differentiating into lineage-specific colonies *in vitro*. Additionally, another population has been categorized as LSCs ($ALDH^+SSC^{lo}CD45^{lo}Neu5,9Ac_2$--$GPs^{hi}CD34^+CD38^+CD90^-CD117^-CD133^-$), which in spite of being functionally proficient, having the ability to propagate, lacked the skill to differentiate into morphologically distinct, lineage-specific colonies.

Although stem cell markers like CD34, CD90, CD117 and CD133 have been commonly used to isolate HPCs, the major reason behind the failure is the lack of a universal marker [20, 23–25, 31–33]. Identification and isolation of normal HPCs, solely on the basis of expression of cell surface antigens, is not reliable since the isolated population is heterogeneous, with significant overlap between HSCs and mature progenitors [34]. Additionally, the phenotype of cultured or transplanted stem cells may remain stable despite a decline in functional

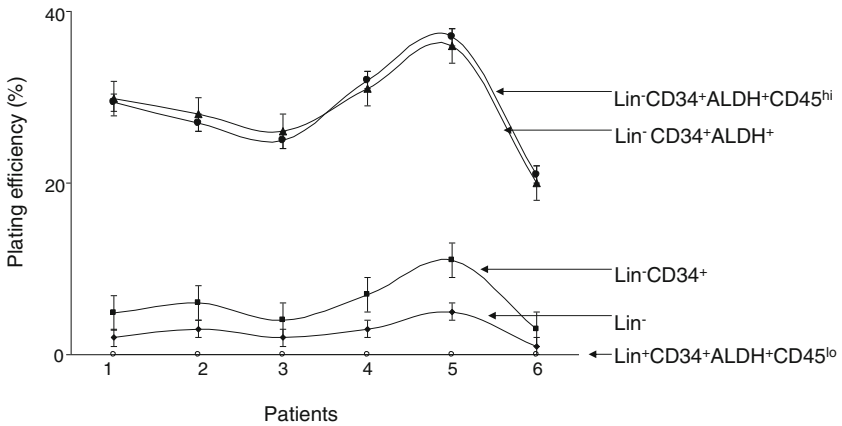

Fig. 5 Plating efficiency of the different sorted populations. Colonies (CFU-E, BFU-E, CFU-G, CFU-M and CFU-GM), produced from culturing different sorted populations, were counted. Plating efficiency was calculated as discussed in Materials and methods and has been shown for triplicate experiments done for six patients labelled 1–6. Plating efficiency of Lin^- (*black diamond*), Lin^-CD^+ (*black square*), $Lin^-CD^+ALDH^+$ (*black triangle*), $Lin^-CD^+ALDH^+CD45^{hi}$ (*black circle*) and $Lin^+CD34^+ALDH^+CD45^{lo}$ (*white circle*) populations for each of the patients have been shown

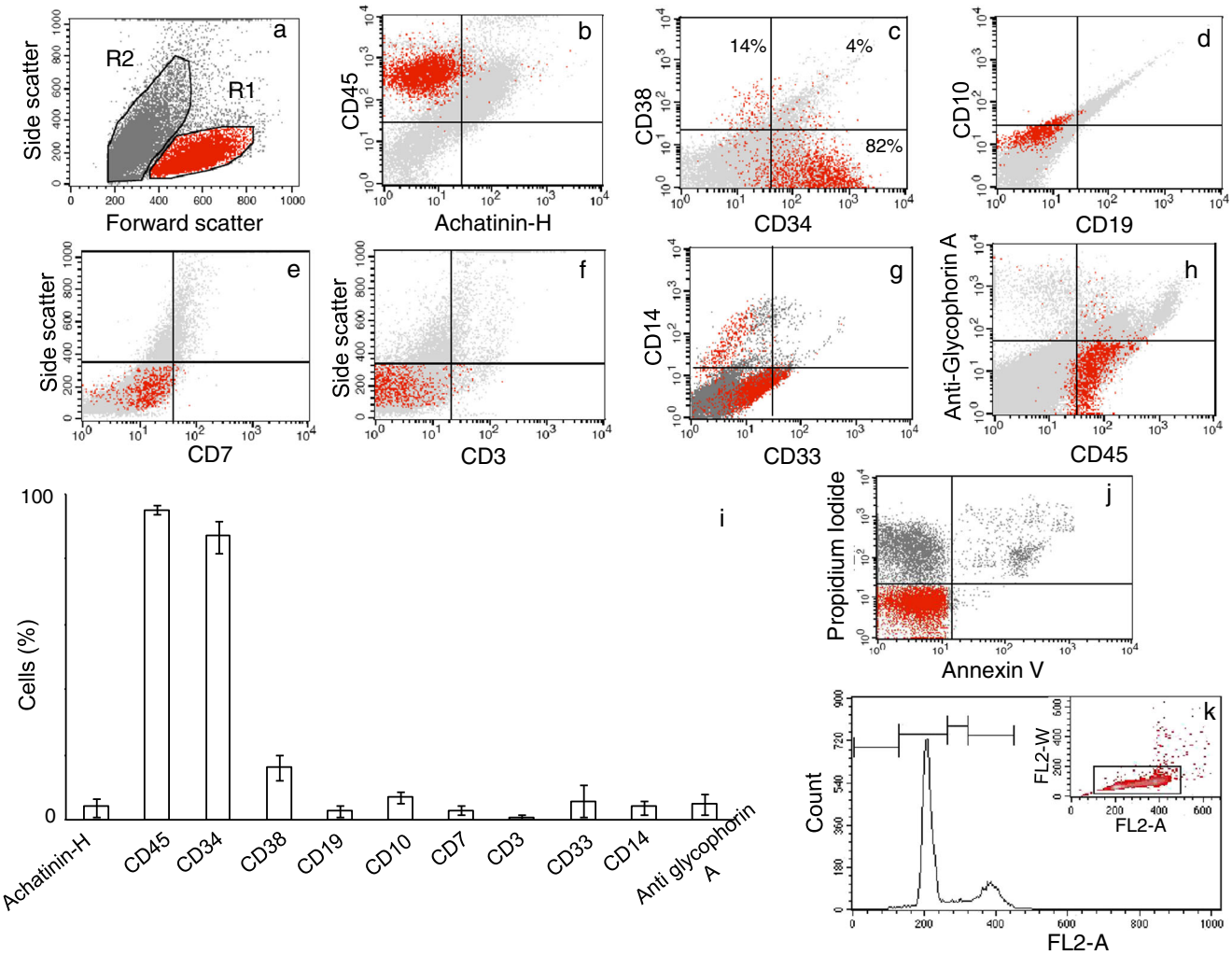

Fig. 6 Determination of lineage content of individual colonies by flow cytometry. Colonies isolated from the culture was washed and assessed for the presence of lineage specific antigens as described in Materials and methods. Results of three colonies differing in their lineage composition are shown. Scatter based on size and granularity showed two populations gated R1 (*red*) and R2 (*grey*) (**a**). Status of Achatinin-H and CD45 (**b**), CD34 and CD38 (**c**), CD19 and CD10 (**d**), CD7 with SSC (**e**), CD3 with SSC (**f**), CD33 and CD14 (**g**) and that of CD45 and anti-Glycophorin A (**h**) are shown using multi-colour dot plots. The column graph showing the percentages of these cell surface markers is shown (**i**). Dot plot with FITC-Annexin V and Propidium iodide shown in (**j**) to gate the alive (R1) and dead (R2) cell population. The DNA cell cycle analysis of R1 is shown in **k**

activity [35, 36]. Populations with phenotypic characteristics of HSCs have been isolated with inability to reconstitute haematopoiesis [37]. Thus it may be envisaged that the need for more stem cell specific biomarkers still exist.

Interestingly, for identification of normal HPCs, the intracellular expression of the developmentally-regulated ALDH is explored [20–25]. An elevated level of cytosolic ALDH is a stringent phenomenon in HPCs [21]. HPCs express highest level of ALDH compared to lymphocytes [22]. Therefore, use of ALDH as a marker not only ensured that the two populations recognized here were primitive, but also constituted of functionally active, viable cells. However, since the progenitor population with high ALDH activity contains both HPCs and LSCs, biomarkers were required for distinguishing between the two.

In this study, we report for the first time an additional cell surface bio-marker, Neu5,9Ac_2-GPs, whose differential expression, identifies a functionally normal HPC population among the lymphoblasts of BM_{ALL}. This identified population has low expression of Neu5,9Ac_2-GPs (Neu5,9Ac_2-GPs^{lo}) with MFI of ~100 au, indicating normal leukocytes, further confirmed by the elevated expression of CD45. This Neu5,9Ac_2-GPs^{lo}CD45^{hi} population was CD34$^+$, CD90$^+$, CD117$^+$ and CD133$^+$ and CD38$^-$ attesting to their primitive haematopoietic nature. These cells were functionally active as identified by the high cytosolic ALDH activity, medium FSC and low SSC (SSC^{lo}), which

characterizes the stem/progenitor population. Additionally, this $ALDH^+SSC^{lo}CD45^{hi}Neu5,9Ac_2$--$GPs^{lo}CD34^+CD38^-CD90^+CD117^+CD133^+$ population was capable of forming colonies in metylcellulose-based medium and lineage specific differentiation *in vitro*.

Lineage composition analysis of the colonies showed that they were normal lymphocytes ($Neu5,9Ac_2$-$GPs^{lo}CD45^{hi}$). Few cells were lineage-committed ($CD38^+$) while most were primitive. They expressed myeloid-, monocytic- and erythroid-associated antigens ensuring that this $Neu5,9Ac_2$--GPs^{lo} population have the capacity for complete haematopoietic reconstitution.

In contrast to the normal HPC population, the LSC population with high cytosolic ALDH activity ($ALDH^+SSC^{lo}CD45^{lo}Neu5,9Ac_2$--$GPs^{hi}CD34^+CD38^+CD90^-CD117^-CD133^-$), showed over expression of $Neu5,9Ac_2$-GPs, with MFI >100 au, similar to leukemic blasts. They were $CD45^{lo}$, a feature distinguishing the leukemic blasts from normal lymphocytes [26–28]. These cells lacked CD90, CD117 and CD133 but co-expressed CD34 and CD38, indicating that they were lineage-committed. Therefore, these cells could well be identified as leukemic cells. However, since high ALDH activity distinguishes progenitor cells from normal haematopoietic cells, this population of cells might be the cancer stem cell population. As expected, this population did not yield any morphologically different colony in *in vitro* clonogenic assay, assuring that these were not the normal HPCs.

The LSC population showing higher expression of $Neu5,9Ac_2$-GPs indicated that the transformation and enhancement occurred in the progenitor LSC population. The lineage-committed status ($CD38^+$) of the LSC might be contrary to the concept of stem cells being lineage negative. However, some form of normal stem or progenitor cell undergoes a mutation, giving rise to an entity that is functionally defined as LSC. These mutated stem cells have properties similar to normal stem cells with respect to self-renewal but they differentiate into the haematopoietic lineage carrying the defect/s and accumulate as immature progenitor cells, also known as blast cells [38], justifying the $CD38^+$ phenotype of LSCs.

The progenitor populations, having high cytosolic ALDH levels, are cyclophosphamide resistant [21–23, 25]. The intracellular level of ALDH is directly related to cellular resistance to activated cyclophosphamide and is important in the survival of cells capable of repopulating marrow in autologous BM transplants. The unique position of activated cyclophosphamide in purging regimens for autologous BM transplant is based on its ability to selectively spare immature haematopoietic cells [22]. The most primitive haematopoietic cells contain relatively high levels of ALDH that potentially protect them against activated cyclophosphamide in tumour cell purging regimen and *in vivo*.

However, this phenomenon has a reverse side. In addition to the HPCs, the LSCs express ALDH with same intensity. This is why both the HPCs and LSCs escape chemotherapy [21]. While the survival of the normal HPCs is for the benefit of the patients, the co-existence of LSCs as minimal residual disease (MRD) might be a major cause of relapse and mortality [38].

To the best our knowledge, this is the first report for the existence of LSCs in childhood ALL. Using the differential expression of $Neu5,9Ac_2$-GPs, being low for the normal HPCs and high for the LSCs, along with the aforesaid panel of stem cell antigens, these populations can easily be identified and isolated.

The haematopoietic reconstitution ability of the normal HPCs *in vitro* simulate the prospective *in vivo* scenario in the patients. Therefore, detailed studies on this HPC population regarding their haematopoietic reconstitution ability *in vivo* may help in cytotherapy by autologous BM transplantation.

The LSCs can be an excellent subject for MRD analysis and targeting the eradication of these cells can minimise relapse. Moreover, the high expression of $Neu5,9Ac_2$-GPs on the lymphoblasts plays a role in their survival [39, 40] and that of *O*-acetylated sialoglycoconjugates in maturation of erythrocytes [41]. These expressions are orchestrated by a series of enzymes [42–45]. Therefore, modulating one or more of these enzymes and/or targeting them for drug-targeted immunotherapy might be of help in managing this disease. Such studies are ongoing.

Acknowledgments We sincerely acknowledge CSIR-IICB, CSIR (IAP-0001, HCP004, NMITLI, TLP-004) and DBT (GAP 235), Department of Science and Technology (DST), ICMR Govt. of India New Delhi. CM is grateful to financial support by J.C. Bose Fellowship, DST and mutual grant from ICMR and German Cancer Research Centre. The authors thank Mr. Asish Mullick for his excellent technical assistance. Mr. Chandan Mandal, Mr. Kaushik Bhattacharya and Ms Susmita Mondal are sincerely acknowledged for their help in carrying out some of the experiments.

References

1. Pui, C.H., Campana, D., Evans, W.E.: Childhood acute lymphoblastic leukaemia–current status and future perspectives. Lancet Oncol. **2**, 597–607 (2001). doi:10.1016/S1470-2045(01)00516-2
2. Pui, C.H., Robison, L.L., Look, A.T.: Acute lymphoblastic leukaemia. Lancet **371**, 1030–1043 (2008). 10.1016/S0140-6736(08)60457-2
3. Sallan, S.E.: Myths and lessons from the adult/pediatric interface in acute lymphoblastic leukemia. Hematol. Am. Soc. Hematol. Educ. Program. 128–132 (2006). doi:10.1182/asheducation-2006.1.128
4. Xu, J., Zhou, T., Zhang, Y.: Role of dendritic cells and chemokines in acute graft-versus-host disease. Front. Biosci. **13**, 2065–2074 (2008). 10.2741/2824

5. Schauer, R.: The diversity of sialic acids and their interplay with lectins. Glycobiology **8**, 136–149 (2006)
6. Ghosh, S., Bandyopadhyay, S., Mukherjee, K., Mallick, A., Pal, S., Mandal, C., *et al.*: O-acetylation of sialic acids is required for the survival of lymphoblasts in childhood acute lymphoblastic leukemia (ALL). Glycoconj. J. **24**, 17–24 (2007). doi:10.1007/s10719-006-9007-y
7. Mandal, C., Schwartz-Albiez, R., Vlasak, R.: Functions and biosynthesis of o-acetylated sialic acids. Top. Curr. Chem. (2012). doi:10.1007/128_2011_310
8. Sinha, D., Mandal, C., Bhattacharya, D.K.: A novel method for prognostic evaluation of childhood acute lymphoblastic leukemia. Leukemia **13**(309–312) (1999)
9. Sen, G., Mandal, C.: The specificity of the binding site of Achatinin H, a sialic acid-binding lectin from *Achatina fulica*. Carbohydr. Res. **268**, 115–125 (1995). 10.1016/0008-6215(94)00311-3
10. Basu, S., Mandal, C., Allen, A.K.: Chemical-modification studies of a unique sialic acid-binding lectin from the snail *Achatina fulica.* Involvement of tryptophan and histidine residues in biological activity. Biochem. J. **254**, 195–202 (1988)
11. Mandal, C., Basu, S., Mandal, C.: Physiochemical studies on achatininH, a novel sialic acid-binding lectin. Biochem. J. **257**, 65–71 (1989)
12. Sinha, D., Mandal, C., Bhattacharya, D.K.: Identification of 9-O acetyl sialoglycoconjugates (9-OAcSGs) as biomarkers in childhood acute lymphoblastic leukemia using a lectin, Achatinin H, as a probe. Leukemia **13**, 119–125 (1999)
13. Mandal, C., Chatterjee, M., Sinha, D.: Investigation of 9-O-acetylated sialoglycoconjugates in childhood acute lymphoblastic leukaemia. Br. J. Haematol. **110**, 801–812 (2000). doi:10.1046/j.1365-2141.2000.02105.x
14. Sinha, D., Mandal, C., Bhattacharya, D.K.: Development of a simple, blood based lymphoproliferation assay to assess the clinical status of patients with acute lymphoblastic leukemia. Leuk. Res. **23**, 433–439 (1999). 10.1016/S0145-2126(98)00184-2
15. Sinha, D., Bhattacharya, D.K., Mandal, C.: A colorimetric assay to evaluate the chemotherapeutic response of children with acute lymphoblastic leukemia (ALL) employing achatininH: a 9-O-acetyl sialic acid binding lectin. Leuk. Res. **23**, 803–809 (1999). 10.1016/S0145-2126(99)00093-4
16. Pal, S., Ghosh, S., Bandyopadhyay, S., Mandal, C., Bandyopadhyay, S., Bhattacharya, D.K., *et al.*: Differential expression of 9-O-acetylated sialoglycoconjugates on leukemic blasts: a potential tool for long-term monitoring of children with acute lymphoblastic leukemia. Int. J. Cancer **111**, 270–277 (2004). doi:10.1002/ijc.20246
17. Pal, S., Ghosh, S., Mandal, C., Kohla, G., Brossmer, R., Isecke, R., *et al.*: Purification and characterization of 9-O-acetylated sialoglycoproteins from leukemic cells and their potential as immunological tool for monitoring childhood acute lymphoblastic leukemia. Glycobiology **14**, 859–870 (2004). doi:10.1093/glycob/cwh111
18. Chowdhury, S., Bandyopadhyay, S., Chandra, S., Mandal, C.: Comparative analysis of differential expression of sialic acids and adhesion molecules on mononuclear cells of bone marrow and peripheral blood in childhood acute lymphoblastic leukaemia at diagnosis and clinical remission. Indian J. Biochem. Biophys. **44**, 357–365 (2007)
19. Chowdhury, S., Bandyopadhyay, S., Mandal, C., Chandra, S., Mandal, C.: Flow-cytometric monitoring of disease-associated expression of 9-O-acetylated sialoglycoproteins in combination with known CD antigens, as an index for MRD in children with acute lymphoblastic leukaemia: a two-year longitudinal follow-up study. BMC Cancer **8**, 40 (2008). doi:10.1186/1471-2407-8-40
20. Storms, R.W., Green, P.D., Safford, K.M., Niedzwiecki, D., Cogle, C.R., Colvin, O.M., *et al.*: Distinct hematopoietic progenitor compartments are delineated by the expression of aldehyde dehydrogenase and CD34. Blood **106**, 95–102 (2005). doi:10.1182/blood-2004-09-3652
21. Jones, R.J., Barber, J.P., Vala, M.S., Collector, M.I., Kaufmann, S.H., Ludeman, S.M., *et al.*: Assessment of aldehyde dehydrogenase in viable cells. Blood **85**, 2742–2746 (1995)
22. Kastan, M.B., Schlaffer, E., Russo, J.E., Colvin, O.M., Civin, C.I., Hilton, J.: Direct demonstration of elevated aldehyde dehydrogenase in human hematopoietic progenitor cells. Blood **75**, 1947–1950 (1990)
23. Storms, R.W., Trujillo, A.P., Springer, J.B., Shah, L., Colvin, O.M., Ludeman, S.M., *et al.*: Isolation of primitive human hematopoietic progenitors on the basis of aldehyde dehydrogenase activity. Proc. Natl. Acad. Sci. U. S. A. **96**, 9118–9123 (1999). doi:10.1073/pnas.96.16.9118
24. Hess, D.A., Meyerrose, T.E., Wirthlin, L., Craft, T.P., Herrbrich, P.E., Creer, M.H., *et al.*: Functional characterization of highly purified human hematopoietic repopulating cells isolated according to aldehyde dehydrogenase activity. Blood **104**, 1648–1655 (2004). doi:10.1182/blood-2004-02-0448
25. Pearce, D.J., Taussig, D., Simpson, C., Allen, K., Rohatiner, A.Z., Lister, T.A., *et al.*: Characterization of cells with a high aldehyde dehydrogenase activity from cord blood and acute myeloid leukemia samples. Stem Cells **23**, 752–760 (2005). doi:10.1634/stemcells.2004-0292
26. Jennings, C.D., Foon, K.A.: Recent advances in flow cytometry: application to the diagnosis of hematologic malignancy. Blood **90**, 2863–2892 (1997)
27. Lacombe, F., Durrieu, F., Briais, A., Dumain, P., Belloc, F., Bascans, E., *et al.*: Flow cytometry CD45 gating for immunophenotyping of acute myeloid leukemia. Leukemia **11**, 1878–1886 (1997)
28. Behm, F.G., Raimondi, S.C., Schell, M.J., Look, A.T., Rivera, G.K., Pui, C.H.: Lack of CD45 antigen on blast cells in childhood acute lymphoblastic leukemia is associated with chromosomal hyperdiploidy and other favorable prognostic features. Blood **79**, 1011–1016 (1992)
29. Pal, S., Chatterjee, M., Bhattacharya, D.K., Bandhyopadhyay, S., Mandal, C., Mandal, C.: O-Acetyl sialic acid specific IgM in childhood acute lymphoblastic leukemia. Glycoconjugate J. **18**, 529–537 (2001)
30. Chowdhury, S., Mandal, C., Sarkar, S., Bag, A.K., Vlasak, R., Chandra, S., Mandal, C.: Mobilization of lymphoblasts from bone marrow to peripheral blood in childhood acute lymphoblastic leukaemia: role of 9-O-acetylated sialoglycoproteins. Leuk. Res. **36**, 146–155 (2012). 10.1016/j.leukres.2011.10.017
31. Goodell, M.A., Rosenzweig, M., Kim, H., Marks, D.F., DeMaria, M., Paradis, G., *et al.*: Dye efflux studies suggest that hematopoietic stem cells expressing low or undetectable levels of CD34 antigen exist in multiple species. Nat. Med. **3**, 1337–1345 (1997)
32. Bhatia, M., Bonnet, D., Murdoch, B., Gan, O.I., Dick, J.E.: A newly discovered class of human hematopoietic cells with SCID-repopulating activity. Nat. Med. **4**, 1038–1045 (1998). 10.1038/2023
33. Jones, R.J., Collector, M.I., Barber, J.P., Vala, M.S., Fackler, M.J., May, W.S., *et al.*: Characterization of mouse lymphohematopoietic stem cells lacking spleen colony-forming activity. Blood **88**, 487–491 (1996)
34. Li, C.L., Johnson, G.R.: Rhodamine123 reveals heterogeneity within murine Lin-, Sca-1+ hemopoietic stem cells. J. Exp. Med. **175**, 1443–1447 (1992)
35. Spangrude, G.J., Brooks, D.M., Tumas, D.B.: Long-term repopulation of irradiated mice with limiting numbers of purified hematopoietic stem cells: in vivo expansion of stem cell phenotype but not function. Blood **85**, 1006–1016 (1995)
36. Yonemura, Y., Ku, H., Hirayama, F., Souza, L.M., Ogawa, M.: Interleukin 3 or interleukin 1 abrogates the reconstituting ability of hematopoietic stem cells. Proc. Natl. Acad. Sci. U. S. A. **93**, 4040–4044 (1996)

37. Randall, T.D., Weissman, I.L.: Characterization of a population of cells in the bone marrow that phenotypically mimics hematopoietic stem cells: resting stem cells or mystery population? Stem Cells **16**, 38–48 (1998). doi:10.1002/stem.160038
38. Jordan, C.T.: The leukemic stem cell. Best Pract. Res. Clin. Haematol. **20**, 13–18 (2007). 10.1016/j.beha.2006.10.005
39. Ghosh, S., Bandyopadhyay, S., Mallick, A., Pal, S., Vlasak, R., Bhattacharya, D.K., *et al.*: Interferon gamma promotes survival of lymphoblasts over expressing 9-O-acetylated sialoglycoconjugates in childhood acute lymphoblastic leukaemia (ALL). J. Cell. Biochem. **95**, 206–216 (2005). doi:10.1002/jcb.20382
40. Ghosh, S., Bandyopadhyay, S., Pal, S., Das, B., Bhattacharya, D.K., Mandal, C.: Increased interferon gamma production by peripheral blood mononuclear cells in response to stimulation of overexpressed disease-specific 9-O-acetylated sialoglycoconjugates in children suffering from acute lymphoblastic leukaemia. Br. J. Haematol. **128**, 35–41 (2005). doi:10.1111/j.1365-2141.2004.05256.x
41. Mukherjee, K., Chowdhury, S., Mondal, S., Mandal, C., Chandra, S., Bhadra, R.K., *et al.*: 9-O-acetylated GD3 triggers programmed cell death in mature erythrocytes. Biochem. Biophys. Res. Commun. **362**, 651–657 (2007). 10.1016/j.bbrc.2007.08.048
42. Mandal, C., Srinivasan, G.V., Chowdhury, S., Chandra, S., Mandal, C., Schauer, R., *et al.*: High level of sialate-O-acetyltransferase activity in lymphoblasts of childhood acute lymphoblastic leukaemia (ALL): enzyme characterization and correlation with disease status. Glycoconjugate J. **26**, 57–73 (2008)
43. Srinivasan, G.V., Schauer, R. Assays of sialate-O-acetyltransferases and sialate-O-acetylesterases. Glycoconjugate J. 2008
44. Mandal, C., Tringali, C., Mondal, S., Anastasia, L., Chandra, S., Venerando, B., Mandal, C.: Down regulation of membrane-bound Neu3 constitutes a new potential marker for childhood acute lymphoblastic leukemia and induces apoptosis suppression of neoplastic cells. Int. J. Cancer **126**, 337–349 (2010). doi:10.1002/ijc.24733
45. Mandal, C., Mandal, C., Chandra, S., Schauer, R., Mandal, C.: Regulation of O-acetylation of sialic acids by sialate-O-acetyltransferase and sialate-O-acetylesterase activities in childhood acute lymphoblastic leukemia. Glycobiology **22**, 70–83 (2012). doi:10.1093/glycob/cwr106